

Supplemental experimental procedures

Digital imaging fluorescence microscopy

Cytospins were fixed for 10 min with 4% of paraformaldehyde (PFA), permeabilized for 10 min with 0.1% of Triton-X followed by blocking with 10% fetal calf serum (FCS) for 1 h. Nuclei were stained with 4',6-diamidino-2-phenylindole (DAPI). Images were obtained using the the Zeiss Axiovert 200M Marianas™ inverted microscope connected to a Cooke Sensicam SVGA CCD camera (Cooke Co., Tonawanda, NY). Data acquisition and processing was performed using SlideBook™ software (SlideBook™ version 5.5.2.0, [Intelligent Imaging Innovations, Denver, CO]).

Supplemental Tables

Supplemental Table S1. Characteristics of high AAI and low AAI AML patients.

Patient characteristics	High AAI	Low AAI
FAB classification	n (%)	n (%)
M0	2 (7.1)	2 (6.5)
M1	5 (17.9)	3 (9.7)
M2	5 (17.9)	7 (22.6)
M3	0 (0)	2 (6.5)
M4	3 (10.7)	7 (22.6)
M5	8 (28.6)	5 (16.2)
M6	1 (3.6)	1 (3.2)
Raeb-t	2 (7.1)	3 (9.7)
Unclassified	2 (7.1)	1 (3.2)
Cytogenetics		
Favorable	3 (10.7)	4 (12.9)
Intermediate	13 (46.4)	19 (61.3)
Poor	4 (14.3)	2 (6.5)
Not available	8 (28.6)	6 (19.4)
Gender		
Female	12 (42.9)	20 (64.5)
Male	16 (57.1)	11 (35.5)
Age median (range)	52 (19-77)	62 (23-76)

Supplemental Table S2. Expression of apoptosis-related proteins in lymphocytes from AML BM at diagnosis and normal BM (nBM).

	AML mean \pm SD	AML median (range)	nBM mean \pm SD	nBM median (range)	Significance
BCL-2	23.4 \pm 13.8	24.2 (2.8-56.6)	11.1 \pm 4.2	10.7 (3.8-19)	0.016
BCL-XL	3.1 \pm 2.2	2.7 (0.6-11.8)	2.9 \pm 1.1	2.6 (1.4-4.5)	0.714
MCL-1	6.7 \pm 3.8	6.8 (0.9-23.4)	5.5 \pm 2.3	4.8 (3.1-10.5)	0.197
BAX	3.1 \pm 2.8	2.4 (0.6-16.3)	3.2 \pm 1.1	3.7 (1.6-4.9)	0.167

Supplemental Table S3. Overview of high AAI and low AAI AML patients used in contact cultures and proteomics experiments.

	AML samples used	AAI at diagnosis	Bcl-2 at diagnosis	Contact cultures	The whole secretome analysis	Exosome analysis
High AAI	AML 1	220.3	18.8	+	+	-
	AML 2	316	15.1	+	+	+
	AML 3	374.4	24	+	+	-
	AML 4	687.4	21.8	+	+	-
	AML 5	631.4	18.9	+	-	-
	AML 6	222.9	16	+	+	-
Low AAI	AML 7	15.8	3.6	+	+	+
	AML 8	14.3	2.6	+	+	-
	AML 9	34.6	11.5	+	+	-
	AML 10	2.1	2.7	-	+	-
	AML 11	3.6	4.8	-	+	-
	AML 12	4	4.8	-	+	-
	AML 13	17.8	5	+	-	-
	AML 14	20.6	4.5	+	-	-
	AML 15	1.6	5.8	+	-	-
	AML 16	3	2.2	+	-	-

Supplemental Table S4. Spontaneous changes in BCL-2 expression in high and low AAI samples. BCL-2 expression (MFI) in a panel of high AAI and low AAI patient samples measured in freshly isolated cells upon diagnosis, upon thawing samples (for contact cultures or secretome production) and after 24 h incubation in culture media.

	Sample	BCL-2 at diagnosis	BCL-2 upon thawing	BCL-2 after 24 h of incubation
High AAI	AML18	15.2	25.5	37.5
	AML19	33.1	51.2	50.3
	AML21	21.9	78.9	42.0
	AML22	27.4	60.0	67.4
Low AAI	AML17	3.6	26.4	24.4
	AML20	5.2	49.6	32.3

Supplemental Table S7. Top 39 proteins upregulated in the secretome of low AAI AML patients in comparison to high AAI AML patients.

Protein description	Human gene symbol	Mean spectral count		Fold Change*	p value
		Low AAI	High AAI		
Transmembrane emp24 domain-containing protein 7	TMED7	2.26	0.00	∞	0.000
Cathepsin H	CTSH	1.79	0.00	∞	0.005
Keratin, type II cuticular Hb4	KRT84	2.36	0.00	∞	0.007
Calpain-2 catalytic subunit	CAPN2	1.92	0.00	∞	0.011
Isoform 14 of Dysferlin	DYSF	0.92	0.00	∞	0.014
Neutrophil gelatinase-associated lipocalin	LCN2	0.92	0.00	∞	0.021
Isoform 1 of Dynamin-2	DNM2	1.19	0.00	∞	0.023
dolichyl-diphosphooligosaccharide-protein glycosyltransferase precursor	DDOST	1.73	0.00	∞	0.026
Platelet basic protein	PPBP	3.91	0.00	∞	0.028
Vacuolar protein sorting-associated protein 26B	VPS26B	1.47	0.00	∞	0.031
C-C motif chemokine 3	CCL3	2.03	0.00	∞	0.032
Isoform 2 of Cytochrome b5	CYB5A	0.96	0.00	∞	0.035
Galectin-3	LGALS3	12.48	0.16	79.38	0.006
Coagulation factor XIII A chain	F13A1	8.36	0.47	17.73	0.018
Eosinophil lysophospholipase	CLC	1.89	0.16	11.92	0.046
Isoform 1 of Scavenger receptor cysteine-rich type 1 protein M130	CD163	3.06	0.31	9.77	0.048
Lysosomal Pro-X carboxypeptidase	PRCP	3.49	0.47	7.43	0.001
Serpin B10	SERPINB10	11.40	1.57	7.27	0.013
47 kDa protein	HP	8.42	1.17	7.16	0.015
Ectonucleotide pyrophosphatase/phosphodiesterase family member 4	ENPP4	1.56	0.31	4.97	0.025
Maltase-glucoamylase, intestinal	MGAM	4.89	1.25	3.90	0.006
Putative uncharacterized protein DKFZp686P15220	IGHG1	9.05	2.36	3.83	0.015
Putative uncharacterized protein TOR1AIP1	TOR1AIP1	4.10	1.17	3.50	0.003
Keratin, type II cytoskeletal 6A	KRT6A	3.62	1.04	3.49	0.007
Fructose-1,6-bisphosphatase 1	FBP1	19.42	5.61	3.46	0.006
Ferritin	FTL	43.65	15.74	2.77	0.024
Dipeptidyl-peptidase 2	DPP7	14.73	5.39	2.74	0.050
Succinyl-CoA:3-ketoacid-coenzyme A transferase 1, Mitochondrial	OXCT1	6.32	2.34	2.70	0.032
Azurocidin	AZU1	12.16	4.66	2.61	0.010
HSPA5 protein	HSPA5	87.30	36.06	2.42	0.003
Non-secretory ribonuclease	RNASE2	27.32	11.44	2.39	0.006
Endoplasmin	HSP90B1	13.89	5.92	2.35	0.025
Prolyl endopeptidase	PREP	8.80	3.76	2.34	0.042
Protein disulfide-isomerase	P4HB	31.06	13.81	2.25	0.021
N(4)-(beta-N-acetylglucosaminy)-L-asparaginase	AGA	12.11	5.57	2.17	0.036
Glutathione synthetase	GSS	16.30	7.63	2.13	0.012
Isoform 1 of Leukotriene A-4 hydrolase	LTA4H	43.51	21.50	2.02	0.047
Isocitrate dehydrogenase [NADP] cytoplasmic	IDH1	10.74	5.33	2.01	0.015
cDNA FLJ53927, highly similar to Beta-hexosaminidase alpha chain	HEXA	8.28	4.12	2.01	0.027

* - ∞ - unique protein

Supplemental Figures

Supplemental Figure S1. Functional clusters of proteins upregulated in the lysates of high AAI and low AAI primary AML cells. The figure depicts top 5 functional protein clusters identified by Cluster ONE analysis in interaction networks generated in STRING and visualized in Cytoscape. Nodes correspond to upregulated proteins and edges symbolize physical or functional associations. Blue clusters represent proteins upregulated in whole cell lysate of apoptosis-resistant (high AAI) AML cells and green clusters correspond to proteins upregulated in whole cell lysate of apoptosis-sensitive (low AAI) AML blasts. Representative GO terms identified by BiNGO analysis in both high and low AAI AML samples are listed together with the number of proteins (nodes) per cluster and their significance.

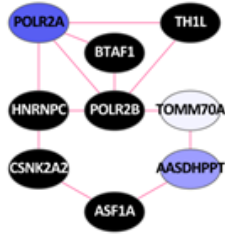
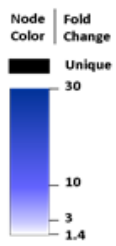
Supplemental Figure S2. Exosome markers enriched in the purified extracellular vesicles fraction of the secretome. The number of spectral counts is shown for 10 different exosome markers detected in purified extracellular vesicle fraction as well as in soluble secretome of the analyzed high AAI and low AAI patient samples.

Supplemental Figure S3. Confocal images of high AAI AML cells-derived EVs uptake. The figure depicts the overall PKH67 uptake in HeLa and low AAI AML cells. HeLa cells after contact culture with PKH67-stained high AAI AML cells show high PKH67 uptake, in contrast to control HeLa cells displaying no PKH67 signal. Similarly, low AAI AML cells show PKH67 signal after incubation with high AAI AML-derived PKH67 stained-EVs, as opposed to control low AAI AML cells.

Supplemental Figure S4. PKH67-stained vesicle uptake in HeLa and low AAI AML cells. PKH67 uptake in HeLa and low AAI AML cells was imaged using digitally enhanced fluorescent microscope. The first 2 panels depict control HeLa cells (incubated without EVs) as well as HeLa upon a 4 h incubation with purified PKH67-stained EVs secreted by high AAI AML cells. In contrast to control HeLa cells displaying no PKH67 signal, the cells incubated with purified EVs are clearly positive for this marker. Similarly, low AAI AML cells incubated for 24 h with the cultured medium, obtained from a 24 h culture of PKH67-stained high AAI AML cells, show bright signal corresponding to PKH67 (panel 3). The last panel (panel 4) depicts the positive control (an ALL cell line CCRF-CEM stained with PKH67), characterised by very high signal intensity of PKH67 signal. This shows that recipient cells, which took EVs up can be distinguished from PKH67-stained cells with high confidence.

Supplemental Figure S1

High AAI



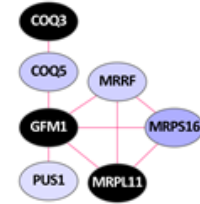
1. RNA processing, transcription, 9 nodes (p=1.82E-04)



2. Mitotic cell cycle, 12 nodes (p=1.85E-04)



3. Ribosome biogenesis, translation, 7 nodes (p=1.0E-03)

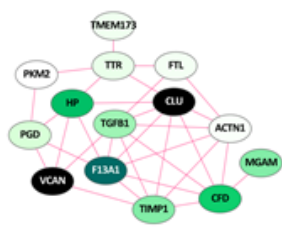
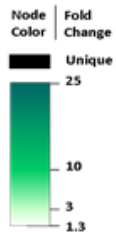


4. Translation, 7 nodes (p=1.4E-03)

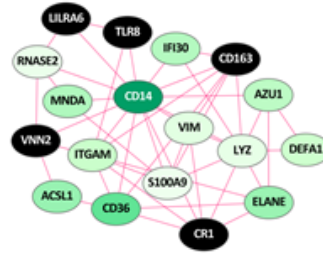


5. Cell adhesion, cell junction formation, 6 nodes (p=3.6E-03)

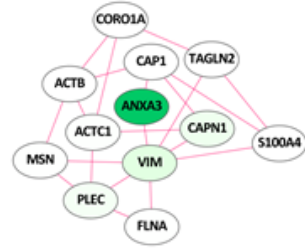
Low AAI



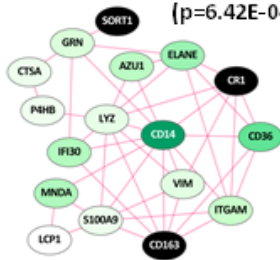
1. Response to stress, innate immune response, 14 nodes (p=6.42E-04)



2. Chemotaxis, response to stimulus, 18 nodes (p=6.96E-04)



3. Actin cytoskeleton organization, 12 nodes (p=3.59E-03)

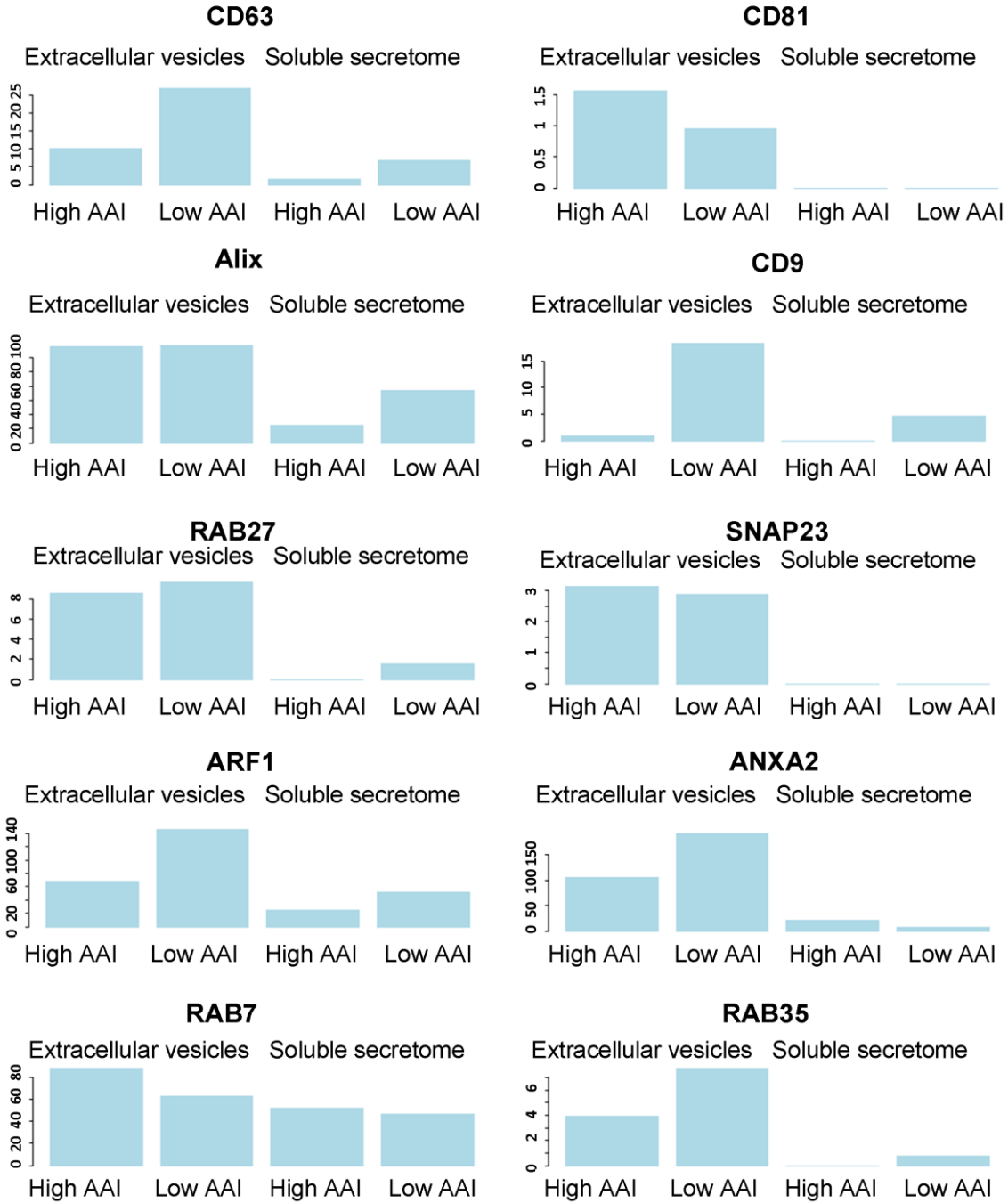


4. Response to stress, defense response (p=1.10E-02)

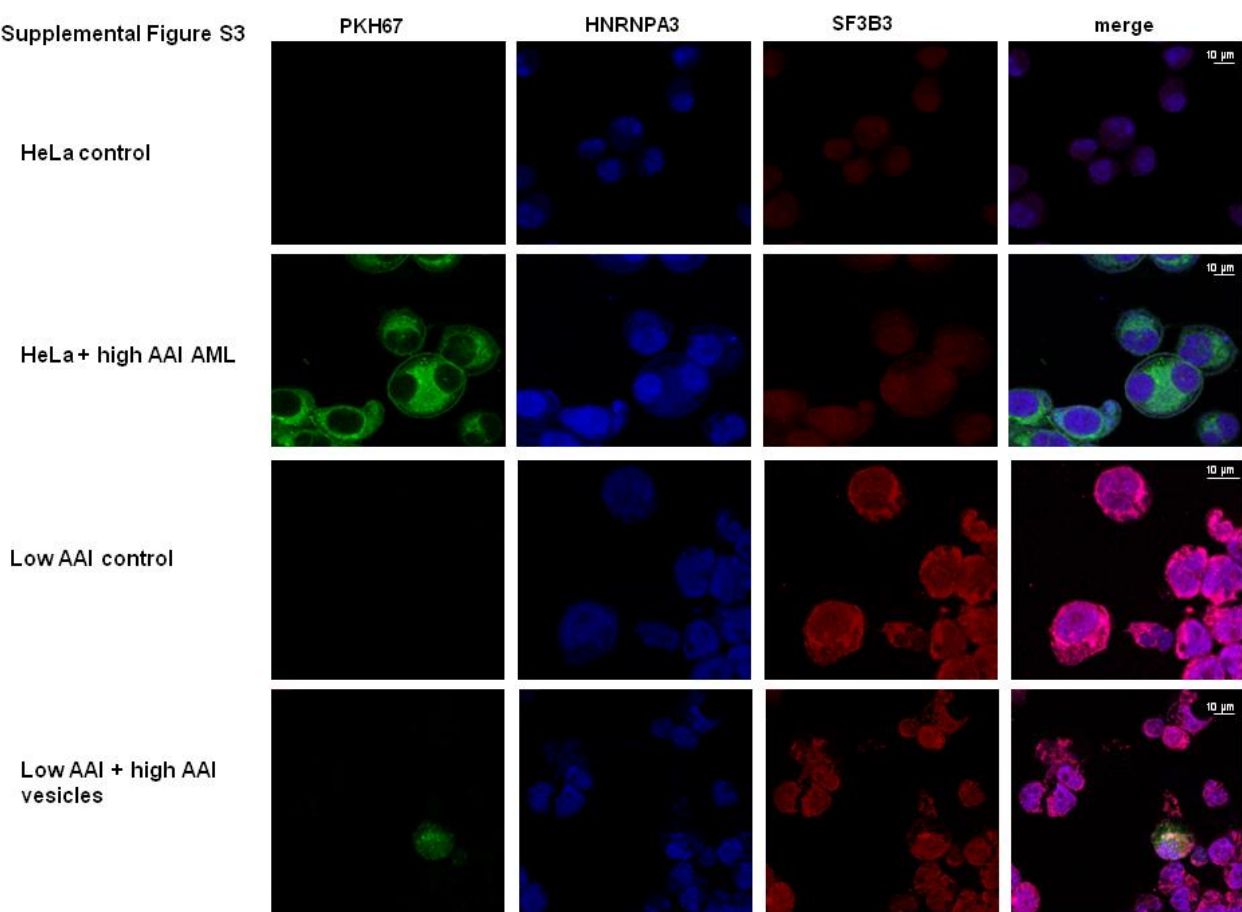


5. Fatty acid metabolic process, 3 nodes (p=2.62E-02)

Supplemental Figure S2



Supplemental Figure S3



Supplemental Figure S4

